A no-hair test for binary black holes

Siddharth Dhanpal,[1,2] Abhirup Ghosh,[1,3] Ajit Kumar Mehta,[1]
Parameswaran Ajith,[1,4] and B. S. Sathyaprakash[5,6]

[1]*International Centre for Theoretical Sciences, Tata Institute of Fundamental Research,*
Bangalore 560012, India
[2]*UM-DAE Centre for Excellence in Basic Sciences, Mumbai 400098, India*
[3]*Max Planck Institute for Gravitational Physics (Albert Einstein Institute),*
D-14476 Potsdam-Golm, Germany
[4]*Canadian Institute for Advanced Research, CIFAR Azrieli Global Scholar, MaRS Centre, West Tower,*
661 University Ave., Suite 505, Toronto, Ontario M5G 1M1, Canada
[5]*Department of Physics and Department of Astronomy and Astrophysics,*
The Pennsylvania State University, University Park, Pennsylvania 16802, USA
[6]*School of Physics and Astronomy, Cardiff University, Cardiff CF24 3AA, United Kingdom*

One of the consequences of the black-hole "no-hair" theorem in general relativity (GR) is that gravitational radiation (*quasinormal modes*) from a perturbed Kerr black hole is uniquely determined by its mass and spin. Thus, the spectrum of quasinormal mode frequencies have to be all consistent with the same value of the mass and spin. Similarly, the gravitational radiation from a coalescing binary black hole system is uniquely determined by a small number of parameters (masses and spins of the black holes and orbital parameters). Thus, consistency between different spherical harmonic modes of the radiation is a powerful test that the observed system is a binary black hole predicted by GR. We formulate such a test, develop a Bayesian implementation, demonstrate its performance on simulated data, and investigate the possibility of performing such a test using previous and upcoming gravitational wave observations.

I. INTRODUCTION

One of the remarkable predictions of general relativity (GR) is that a stationary black hole can be fully described by a small number of parameters—its mass, spin angular momentum, and electric charge [1–3]. As a consequence of this "no-hair" theorem, frequencies of the gravitational radiation (*quasinormal modes* [4–6]) from a perturbed black hole is fully determined by these parameters. Astrophysical black holes are not expected to possess significant electric charge; hence, different quasinormal modes have to be consistent with the same value of the mass and spin. Thus, the consistency between multiple quasinormal modes provides a test of the no-hair theorem for stationary, isolated black holes [7]. Similarly, the dynamics and gravitational radiation from a binary black hole (BBH) system are uniquely determined by a small number of parameters (masses and spins of the black holes and orbital parameters), and hence different spherical harmonic modes of the radiation have to be consistent with the same values of this small set of parameters. Thus, the consistency between different modes of the observed signal is a powerful test that the radiation emanated from a BBH. Inconsistency between different modes would point

to either a departure from GR, or the non-black-hole nature of the compact objects.

Coalescence of binaries composed of chargeless black holes would produce a perturbed Kerr black hole as the remnant, and the late time gravitational-wave (GW) signal is described by a spectrum of quasinormal modes (see, e.g., [8]). While the relatively simple structure of quasinormal modes has been known from black-hole perturbation theory for a long time (see, e.g., [9] for a review), the radiation from the full inspiral, merger, and ringdown have a much more complex structure. Fortunately, recent numerical-relativity simulations, together with high-order analytical calculations, have enabled us to accurately model several subdominant multipoles of the radiation [10–12]. This allows us to formulate a powerful test of the consistency of the GW signal with a BBH waveform in GR, based on the consistency of different multipoles of the radiation. While the relatively low signal-to-noise ratios (SNRs) of the ringdown signals makes the measurement of multiple quasinormal modes extremely difficult using the current generation of GW detectors [13], we show that the test proposed in this paper can be performed using GW detections expected in the next few years, because it makes use of the full inspiral-merger-ringdown signal.

II. TESTING THE CONSISTENCY BETWEEN DIFFERENT MULTIPOLES OF THE GRAVITATIONAL RADIATION

In practice it is difficult to extract different multipoles of the radiation from the GW observation of a single BBH system—all we measure is a particular linear combination of the modes. Thus, our strategy, developed below, is to introduce extra parameters that describe inconsistency between different modes and to constrain them using a Bayesian framework. This is similar in spirit to the tests of the no-hair theorem using quasinormal modes, developed in [14,15].

The two polarizations $h_+(t)$ and $h_\times(t)$ of gravitational radiation in GR can be written as a complex time series $\mathfrak{h}(t) := h_+(t) - ih_\times(t)$, which can be expanded in a basis of spin -2 weighted spherical harmonics [16] as:

$$\mathfrak{h}(t; \mathbf{n}, \boldsymbol{\lambda}) = \frac{1}{d_L} \sum_{\ell=2}^{\infty} \sum_{m=-\ell}^{\ell} Y_{\ell m}^{-2}(\mathbf{n}) \mathfrak{h}_{\ell m}(t; \boldsymbol{\lambda}), \quad (2.1)$$

where $Y_{\ell m}^{-2}$ are the basis functions of spin -2 spherical harmonics, $\mathbf{n} := \{\iota, \varphi_0\}$ define the direction of radiation in the source frame, d_L is the luminosity distance to the binary, and $\mathfrak{h}_{lm}(t; \boldsymbol{\lambda})$ are the spherical harmonic modes of the waveform, which are completely described by the intrinsic parameters $\boldsymbol{\lambda}$ of the system. We assume that the black holes are nonspinning and the binary to be quasi-circular. Hence $\boldsymbol{\lambda}$ consists of only the masses m_1 and m_2 of the black holes (it is more convenient to describe the system in terms of the *chirp mass* $M_c := (m_1 m_2)^{3/5}/(m_1 + m_2)^{1/5}$ and mass ratio $q = m_2/m_1 \leq 1$). In GR, the gravitational radiation is dominated by the quadrupole modes ($\ell = 2, m = \pm 2$); however nonquadrupole modes can make an appreciable contribution if the black holes have significantly unequal masses. The set of intrinsic parameters $\boldsymbol{\lambda} := \{M_c, q\}$ completely determines the multipolar structure (i.e., spherical harmonic modes) of the waveform $\mathfrak{h}_{lm}(t)$.

In order to formulate a consistency test between different multipoles, we rewrite Eq. (2.1) by splitting the contributions from the dominant ($\ell = 2, m = \pm 2$) mode of gravitational radiation, and the subdominant (higher order) modes

$$\mathfrak{h}(t; \mathbf{n}, \boldsymbol{\lambda}, \Delta\boldsymbol{\lambda}) = \sum_{m=\pm 2} Y_{2m}^{-2}(\mathbf{n}) \mathfrak{h}_{2m}(t, \boldsymbol{\lambda})$$
$$+ \sum_{\text{H.O.M}} Y_{\ell m}^{-2}(\mathbf{n}) \mathfrak{h}_{\ell m}(t, \boldsymbol{\lambda} + \Delta\boldsymbol{\lambda}) \quad (2.2)$$

where the sum in the second term on the right-hand side (RHS) is just over the higher-order modes. Note that we allow a possibility of inconsistency between the dominant mode and higher order modes by introducing a deviation $\Delta\boldsymbol{\lambda} := \{\Delta M_c, \Delta q\}$ in the set of intrinsic parameters that describe the higher-order modes. For BBHs in GR, $\Delta\boldsymbol{\lambda} = 0$.

An interferometric GW detector observes a linear combination of the two polarizations $h_+(t)$ and $h_\times(t)$, given by

$$h(t) = F_+(\theta, \phi, \psi) h_+(t - t_0) + F_\times(\theta, \phi, \psi) h_\times(t - t_0), \quad (2.3)$$

where F_+ and $F_\times$ are the antenna pattern functions of the GW detector, t_0 is the time of arrival of the signal at the detector, and $(\theta, \phi), \psi$ define the sky position and polarization angle of the GW source, respectively. For coalescing BBH systems in quasicircular orbits, the observed signal $h(t)$ is described by a set of *intrinsic* parameters $\boldsymbol{\lambda} = \{M_c, q\}$ and *extrinsic* parameters $\boldsymbol{\theta} := \{t_0, \iota, \varphi_0, d_L, \theta, \phi, \psi\}$ in GR. In addition to the parameters that describe signals in GR, we introduce a set of parameters $\Delta\boldsymbol{\lambda}$ describing difference between the intrinsic parameters used to generate the dominant and subdominant modes. The combined set of parameters is denoted as $\boldsymbol{\xi} = \{\boldsymbol{\lambda}, \boldsymbol{\theta}, \Delta\boldsymbol{\lambda}\}$.

The data $d(t) = n(t) + h(t)$ contains the observed signal $h(t)$ given in Eq. (2.3) along with noise $n(t)$, which is modeled as a stationary Gaussian random process. Given data d and assuming a particular model of the waveform given in (2.2) as our hypothesis H, we can compute the posterior distribution of the set of parameters $\boldsymbol{\xi}$ making use of the Bayes theorem:

$$P(\boldsymbol{\xi}|d, H) = \frac{P(\boldsymbol{\xi}|H) P(d|\boldsymbol{\xi}, H)}{P(d|H)}. \quad (2.4)$$

The *posterior* probability density $P(\boldsymbol{\xi}|d, H)$ that the data contains a signal with parameters $\boldsymbol{\xi}$ is determined by the *prior* probability distribution $P(\boldsymbol{\xi}|H)$ and the *likelihood* $P(d|\boldsymbol{\xi}, H)$ that the data contains a signal described by parameters $\boldsymbol{\xi}$; $P(d|H)$ is a normalization constant, called the *evidence*. For stationary Gaussian noise with power spectral density $S_n(f)$, the likelihood can be written as:

$$P(d|\boldsymbol{\xi}, H) = \exp\left[-\frac{1}{2} \int_{f_{\text{low}}}^{f_{\text{high}}} \frac{|\tilde{d}(f) - \tilde{h}(f; \boldsymbol{\xi}, H)|^2}{S_n(f)} df\right], \quad (2.5)$$

where f_{low} and f_{high} define the sensitivity bandwidth of the detector, while $\tilde{d}(f)$ and $\tilde{h}(f)$ are the Fourier transforms of $d(t)$ and $h(t)$, respectively.

We estimate the posterior of $\boldsymbol{\xi}$ by stochastically sampling the likelihood function over the entire parameter space of interest. In this work, we use the EMCEE [17] package, a PYTHON implementation of the stochastic sampling algorithm proposed by [18].[1] From the posterior distribution

---

[1] We have compared the posterior distributions obtained from our EMCEE based code with that from the Nested-Sampling based LALINFERENCENEST code [19] that is part of the LIGO Algorithm Library (LAL) software suite [20]. Posteriors obtained from simulated GR waveforms containing only the dominant ($\ell = 2, m = \pm 2$) modes observed by a single detector are in good agreement.

$P(\xi|d, H)$ of the full parameter set, we construct the posterior distribution $P(\Delta\lambda|d, H)$ of the set of parameters $\Delta\lambda := \{\Delta M_c, \Delta q\}$ describing deviation from the GR prediction of a BBH signal, by marginalizing the posterior over all other parameters $\{\lambda, \theta\}$. If the data is consistent with a BBH signal in GR, we expect $P(\Delta\lambda|d, H)$ to be consistent with zero.

III. SIMULATIONS USING BBH WAVEFORMS IN GR

We now demonstrate this test on simulated GW observations of BBH signals predicted in GR. We employ the recent inspiral-merger-ringdown waveform model proposed by [12], which provide accurate Fourier-domain models of the following spherical harmonic modes $\mathfrak{h}_{\ell m}(f)$ of the expected GW signals from nonspinning BBHs: $(\ell = 2, m = \pm 2)$, $(\ell = 2, m = \pm 1)$, $(\ell = 3, m = \pm 3)$, $(\ell = 4, m = \pm 4)$. (The other spherical harmonic modes

FIG. 2. The figure shows the width of the 90% credible region of ΔM_c and Δq for binaries with different mass ratios q (horizontal axis) and inclination angles ι (legends). All binaries have a total mass $40\,M_\odot$. Best constraints are provided by binaries with high mass ratios and/or large inclination angles.

that are neglected only introduce an inaccuracy (mismatch) of less than 1% in the waveforms [12]). GW observations are simulated making use of Eqs. (2.1) and (2.3). For estimating the parameters, we assume the likelihood function given in Eq. (2.5), with noise power spectral density anticipated in Advanced LIGO's "high-power, zero-detuning" configuration [21]. We consider binaries with total mass $M := m_1 + m_2$ in the range $40\,M_\odot$–$200\,M_\odot$ with mass ratio $q := m_2/m_1$ in the range $1/9$–1, with varying inclination angles ι (angle between the orbital angular momentum of the binary and the line of sight).

We perform the test by introducing variations in the higher order modes, as in Eq. (2.2). The higher-order modes $\mathfrak{h}_{\ell m}(f; \lambda + \Delta\lambda)$ are generated by introducing an extra parameter $\Delta\lambda$ while the quadrupole-modes $\mathfrak{h}_{2\pm 2}(f; \lambda)$ are generated by using the standard set of parameters λ in GR. We make two choices for the deviation parameter $\Delta\lambda$: First, by introducing *one* deviation parameter at a time; i.e., $\Delta\lambda = \Delta M_c$ or $\Delta\lambda = \Delta q$. Second, by introducing a concurrent deviation in *two* parameters $\Delta\lambda = \{\Delta M_c, \Delta q\}$. We show in Fig. 1 the results of the tests performed by varying either one parameter or two parameters, for a binary with total mass $M = 80\,M_\odot$, mass ratio $q = 1/9$, inclination angle $\iota = 60°$ producing an SNR of 25 (SNR in higher modes is ∼10). We see that the posterior probability density for the parameters Δq and ΔM_c are consistent with zero as in GR. As expected, the width of the posterior is smaller when only one deviation parameter is allowed to vary at a time (either ΔM_c or Δq). Figures 2 and 3 show the
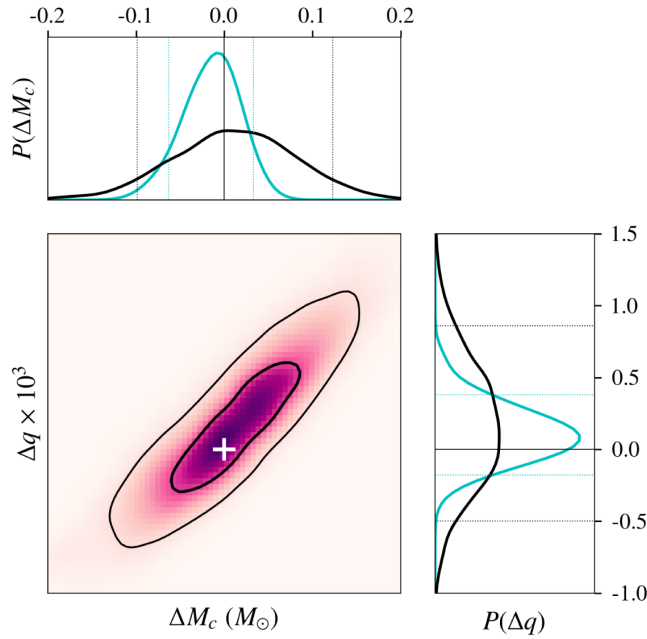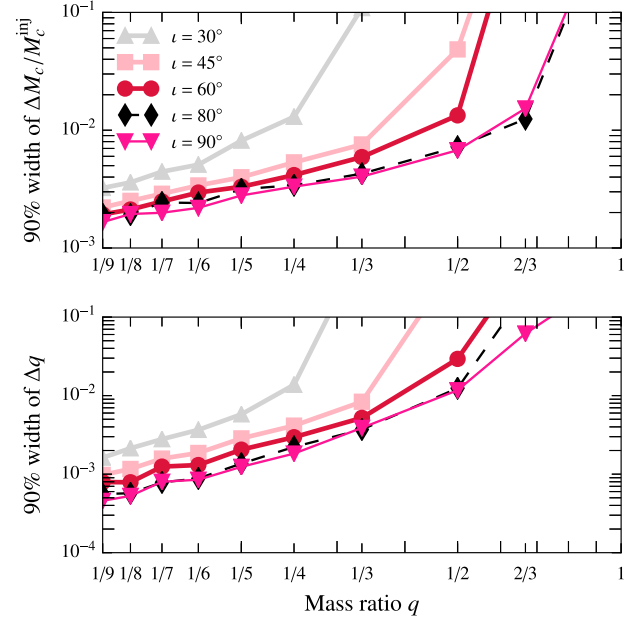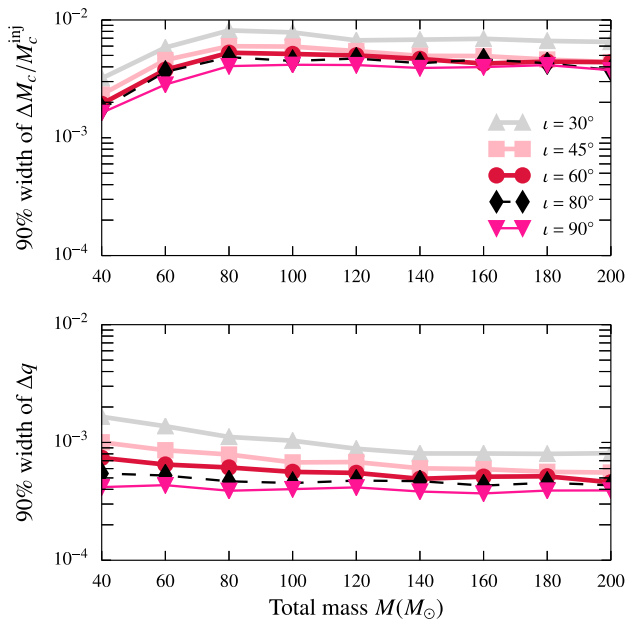

FIG. 1. The thick (thin) contours show the 50% (90%) credible regions in the joint posteriors of two parameters ΔM_c and Δq (difference in the chirp mass M_c and mass ratio q estimated from the quadrupole vs nonquadrupole modes) from a simulated BBH signal. Black histograms on the side panels show the marginalized posteriors in ΔM_c and Δq, while the cyan histograms show the 1-dimensional posteriors in ΔM_c and Δq estimated from the data by introducing only one variation (say, ΔM_c) at a time, keeping the other fixed (say, $\Delta q = 0$). It can be seen that the posteriors are fully consistent with the GR prediction of $\Delta M_c = \Delta q = 0$ (shown by a "+" sign in the center panel and by thin black lines in side panels). In the side panels, the dotted lines mark the 90% credible regions. The simulated GR signal corresponds to a BBH system with total mass $M = 80\,M_\odot$, mass ratio $q = 1/9$ and inclination angle $\iota = 60°$ observed by a single Advanced LIGO detector with an optimal SNR of 25.

FIG. 3. Same as Fig. 2, except that the horizontal axis reports the total mass M. All binaries correspond to a mass ratio $q = 1/9$.

90% credible regions of the posteriors of the deviation parameters for the case of binaries with different masses, mass ratios, and inclination angles. For all cases SNR is 25, and either ΔM_c or Δq is introduced at a time. This shows that binaries with large mass ratios ($q < 1/2$) and inclination angles ($\iota > 60°$) will allow precision tests of the GR predictions, reaching statistical uncertainties $< 10^{-2}$ for $\Delta M_c/M_c$ and Δq.

IV. SIMULATIONS USING NON-BBH WAVEFORMS

If the multipole structure of the GW signal is sufficiently different from that of BBHs in GR (either when the underlying theory is different from GR or when the binary contains compact objects other than black holes), then this test should be able to identify this difference. We demonstrate this by performing the test on a simulated GW signal from a black hole-neutron star binary with mass ratio 1/6 from the numerical-relativity waveform catalog of the SXS collaboration [22]. We rescale this waveform to a total mass of $M = 120\ M_\odot$ and use it as a proxy for GW signals from a binary consisting of at least one non-black hole compact object.[2] Figure 4 shows the posteriors of the deviation parameters ΔM_c and Δq estimated from a simulated observation containing this signal, which are *inconsistent* with the GR prediction of BBHs. The figure

---

[2]Note that the rescaled signal will not correspond to a black hole-neutron star binary, as $m_2 \simeq 17\ M_\odot$ is much larger than the maximum mass of a neutron star. However, we use this as a proxy for GW signals produced by a binary containing an exotic compact object.
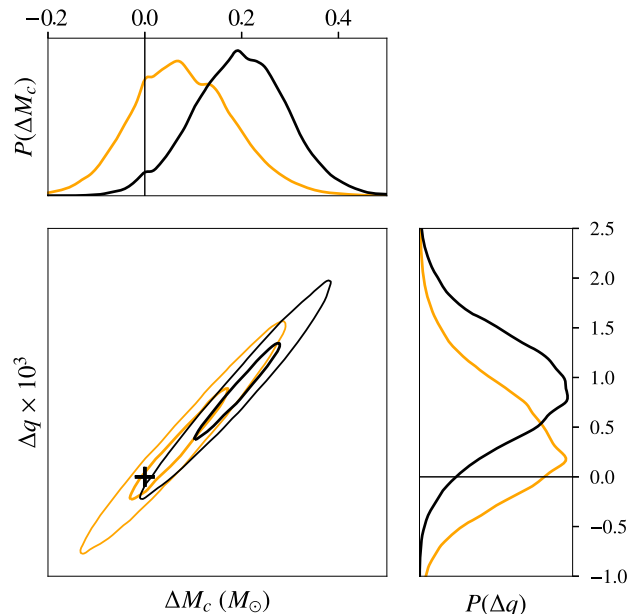

FIG. 4. Black contours show the posterior distributions of ΔM_c and Δq (similar to Fig. 1) estimated from a simulated GW signal from a binary containing at least one compact object other than a black hole. The signal was produced by rescaling a numerical relativity waveform from a neutron star-black hole binary with mass ratio 1/6 to a total mass of 120 $M_\odot$ (inclination angle $\iota = 90°$, producing SNR of 50 in Advanced LIGO). Note that the posteriors are inconsistent with a BBH system in GR ($\Delta M_c = \Delta q = 0$, marked by a "+" sign, is outside the 90% credible region). The orange contours show the posteriors estimated from a numerical relativity waveform from a BBH system with same parameters, which show consistency with $\Delta M_c = \Delta q = 0$.

also shows the results of the test applied on a numerical relativity waveform from a BBH system with same parameters, which shows consistency with $\Delta M_c = \Delta q = 0$. The simulated signals correspond to binaries with inclination angle $\iota = 90°$, producing SNR of 50 in Advanced LIGO.

V. ASTROPHYSICAL PROSPECTS

Recent observations of GW signals from merging binaries of black holes [23–29] and neutron stars [30] by LIGO and Virgo have enabled the first tests of GR in the highly relativistic regime [25–28,31]. However, the test proposed in this paper requires the observation of GW signals where the subdominant modes can be observed with appreciable SNR. These modes are excited predominantly for binaries with large mass ratios. Also, due to the radiation pattern, radiation from binaries with highly inclined orbits will contain appreciable contribution from subdominant modes. Hence binaries with large mass ratios ($q \lesssim 1/2$) and inclined orientations ($\iota \gtrsim 60°$) are particularly suitable sources for performing the test described in this paper. Consequently, we do not expect the test to be
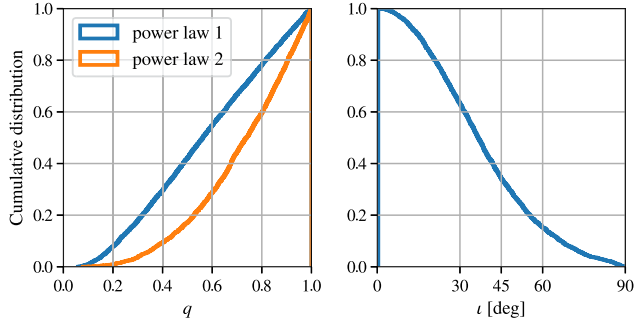
FIG. 5. Projected cumulative distribution of the mass ratio q (left) and inclination angle ι (right) of simulated BBHs that are detectable by Advanced LIGO, based on our assumed component mass distribution. The two distributions in the left plot corresponds to two assumed distributions of the component masses (see text).

effective for GW signals observed by LIGO and Virgo during their first two observational runs, for which mass ratios are less than 2 and inclinations are close to being face-on/face-off [29]. The detection rate of binaries with large mass ratios depends on the astrophysical merger rate of such binaries, which is currently uncertain, while the detection rate of binaries with large inclination angle is related to the same with small inclination angles by a simple geometric factor.

Here we investigate the prospect of performing the proposed test on BBH events that Advanced LIGO and Virgo could observe over the next few years. We simulate populations of BBHs based on reasonable astrophysical assumptions, and examine the distributions of the mass ratio and inclination angle of detectable signals. In particular, we simulate binaries with two astrophysically motivated mass distributions in the source-frame [32]:

(1) Component masses following a power-law $p(m_{1,2}) = m_{1,2}^{-1}$ with $m_1, m_2 \geq 5 \ M_\odot$, and $m_1 + m_2 \leq 100 \ M_\odot$.

(2) Power-law $p(m_1) = m_1^{-2.35}$ on the mass of the larger black hole, with the smaller mass distributed uniformly in q and with $5 \ M_\odot \leq m_1 + m_2 \leq 100 \ M_\odot$.

In both cases, binaries are distributed uniformly in the sky with isotropic orientations. The distribution of the mergers in redshift is chosen according to the prescription given in [33]. The cosmological redshift on the GW signals can be absorbed by a rescaling of the masses $m_{1,2}(1+z)$ where z is the redshift. From the simulated events, we compute the SNR expected in Advanced LIGO and apply an SNR threshold for detection (the probability distributions are independent of the exact value of the SNR threshold). The cumulative distribution of the mass ratio q and inclination angle ι of binaries crossing the detection threshold is plotted in Fig. 5. It can be seen that ∼20–40% of the detectable binaries will have a mass ratio greater than 2, out of which ∼15% will be observed with inclination angle greater than 60°. Thus, only a few percent of the observed systems are likely to have large mass ratios ($q < 1/2$) and
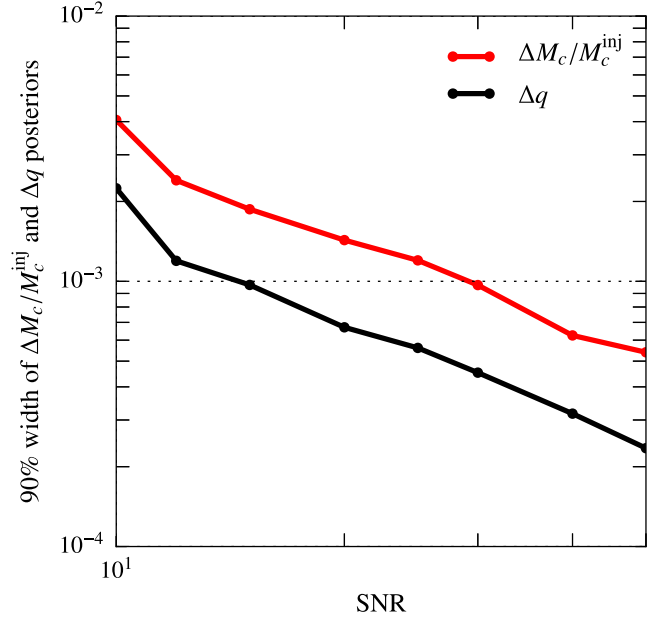

FIG. 6. The width of the 90% credible region of the posteriors of ΔM_c and Δq as a function of the optimal SNR of the signal in a single Advanced LIGO detector. The simulated GR signal corresponds to a BBH system with total mass $M = 80 \ M_\odot$, mass ratio $q = 1/9$, and inclination angle $\iota = 60°$ (same as Fig. 1).

inclined orbits ($\iota > 60°$). However, since Advanced LIGO and Virgo are expected to observe hundreds of BBH mergers over the next few years [32], we conclude that the proposed test could be performed when detectors reach their design sensitivity over the next few years, if not sooner. Indeed, the precision of such tests will depend on the SNR of the observed signals. While the earlier examples that we studied assume a rather high SNR of 25, we show in Fig. 6 that interesting statistical constraints on the deviation parameters can be expected even for modest SNRs, such as 10 or 12.

VI. CONCLUSIONS AND FUTURE WORK

In this paper, we proposed a new method to test the consistency of an observed GW signal with a BBH system predicted by GR. The test relies on the fact that the multipolar structure of the radiated GW signal from a BBH system in quasicircular orbit is uniquely determined in GR by the masses and spins of the black holes and no other parameters. Thus, if we estimate the parameters of the binary from different spherical harmonic modes of the observed signal independently, those estimates will have to be consistent with one another. Any inconsistency between the different estimates will point to a deviation from GR or to the non-black-hole nature of the compact objects. We have used Bayesian parameter inference to identify potential deviations from GR predictions, using simulated GW signals. We provided the first estimates of the expected

precision of such tests that can be performed using GW observations of BBHs anticipated by Advanced LIGO and Virgo in the next few years.

The specific implementation of the test presented in this paper checks for the consistency of the masses (and spins, in the case of spinning binaries) estimated from the quadrupole/nonquadruple modes. If we have enough SNR to distinguish different modes, we can introduce deviation parameters for each mode (say, $\Delta M_c^{\ell m}$ and $\Delta q^{\ell m}$). This is analogous to checking the consistency of different quasinormal mode frequencies, as the frequency evolution of the binary is determined by these intrinsic parameters. In addition, one could also check the consistency of the amplitudes of different modes, by introducing extra parameters describing deviations from the predicted amplitudes. While this would expand the scope of this test, in general, introducing more parameters would increase the statistical uncertainties, due to correlations between different parameters.

We have assumed, for simplicity, that the component black holes of the binary have negligible spins. Nevertheless, the method can be easily generalized to the case of binaries consisting of spinning black holes.

We have also neglected the systematic errors due to inaccuracies in waveform modeling and detector calibration; these need to be understood before implementing the test on real observations. We leave these investigations to future work.

[1] W. Israel, Phys. Rev. **164**, 1776 (1967).
[2] W. Israel, Commun. Math. Phys. **8**, 245 (1968).
[3] B. Carter, Phys. Rev. Lett. **26**, 331 (1971).
[4] C. V. Vishveshwara, Nature (London) **227**, 936 (1970).
[5] W. H. Press, Astrophys. J. **170**, L105 (1971).
[6] S. Chandrasekhar and S. L. Detweiler, Proc. R. Soc. A **344**, 441 (1975).
[7] O. Dreyer, B. J. Kelly, B. Krishnan, L. S. Finn, D. Garrison, and R. Lopez-Aleman, Classical Quantum Gravity **21**, 787 (2004).
[8] A. Buonanno, G. B. Cook, and F. Pretorius, Phys. Rev. D **75**, 124018 (2007).
[9] E. Berti, V. Cardoso, and A. O. Starinets, Classical Quantum Gravity **26**, 163001 (2009).
[10] Y. Pan, A. Buonanno, M. Boyle, L. T. Buchman, L. E. Kidder, H. P. Pfeiffer, and M. A. Scheel, Phys. Rev. D **84**, 124052 (2011).
[11] L. London, S. Khan, E. Fauchon-Jones, C. García, M. Hannam, S. Husa, X. Jiménez-Forteza, C. Kalaghatgi, F. Ohme, and F. Pannarale, Phys. Rev. Lett. **120**, 161102 (2018).
[12] A. K. Mehta, C. K. Mishra, V. Varma, and P. Ajith, Phys. Rev. D **96**, 124010 (2017).
[13] E. Berti, A. Sesana, E. Barausse, V. Cardoso, and K. Belczynski, Phys. Rev. Lett. **117**, 101102 (2016).
[14] S. Gossan, J. Veitch, and B. S. Sathyaprakash, Phys. Rev. D **85**, 124056 (2012).

[15] J. Meidam, M. Agathos, C. Van Den Broeck, J. Veitch, and B. S. Sathyaprakash, Phys. Rev. D **90**, 064009 (2014).
[16] E. T. Newman and R. Penrose, J. Math. Phys. (N.Y.) **7**, 863 (1966).
[17] D. Foreman-Mackey, D. W. Hogg, D. Lang, and J. Goodman, Publ. Astron. Soc. Pac. **125**, 306 (2013).
[18] J. Goodman and J. Weare, Commun. Appl. Math. Comput. Sci. **5**, 65 (2010).
[19] J. Veitch and A. Vecchio, Phys. Rev. D **81**, 062003 (2010).
[20] https://wiki.ligo.org/DASWG/LALSuite.
[21] D. Shoemaker (LIGO Scientific Collaboration), LIGO Document T0900288-v3 (2010).
[22] SXS Gravitational Waveform Database, http://www.black-holes.org/waveforms/.
[23] B. P. Abbott *et al.* (LIGO Scientific and Virgo Collaborations), Phys. Rev. Lett. **116**, 061102 (2016).
[24] B. P. Abbott *et al.* (LIGO Scientific and Virgo Collaborations), Phys. Rev. Lett. **116**, 241103 (2016).
[25] B. P. Abbott *et al.* (LIGO Scientific and Virgo Collaborations), Phys. Rev. X **6**, 041015 (2016).
[26] B. P. Abbott *et al.* (LIGO Scientific and Virgo Collaborations), Phys. Rev. Lett. **118**, 221101 (2017).
[27] B. P. Abbott *et al.* (Virgo and LIGO Scientific Collaborations), Astrophys. J. **851**, L35 (2017).

[28] B. P. Abbott *et al.* (LIGO Scientific and Virgo Collaborations), Phys. Rev. Lett. **119**, 141101 (2017).

[29] B. P. Abbott *et al.* (LIGO Scientific and Virgo Collaborations), arXiv:1811.12907.

[30] B. P. Abbott *et al.* (LIGO Scientific and Virgo Collaborations), Phys. Rev. Lett. **119**, 161101 (2017).

[31] B. P. Abbott *et al.* (LIGO Scientific and Virgo Collaborations), Phys. Rev. Lett. **116**, 221101 (2016).

[32] B. P. Abbott *et al.* (Virgo and LIGO Scientific Collaborations), Astrophys. J. **833**, L1 (2016).

[33] M. Dominik, K. Belczynski, C. Fryer, D. E. Holz, E. Berti, T. Bulik, I. Mandel, and R. O'Shaughnessy, Astrophys. J. **779**, 72 (2013).